

# A Microstrip Directional Coupler with Tight Coupling and Relatively Wideband using Defected Ground Structure

Ayman S. Al-Zayed<sup>1</sup>, Zuhair. M. Hejazi<sup>2</sup>, and Ashraf S. Mohra<sup>2</sup>

<sup>1</sup>Electrical Engineering Department  
Kuwait University, University, P.O. Box 5969, Safat, 13060, Kuwait  
ayman.alzayed@ku.edu.kw

<sup>2</sup>Electrical Engineering Department  
King Saud University, Saudi Arabia  
zhejaz@ksu.edu.sa, amohra@ksu.edu.sa

**Abstract**— This paper presents a detailed investigation utilizing a defected ground structure (DGS) to a conventional edge-coupled microstrip coupler with tight coupling level over a relatively wide frequency band. A reasonable spacing between microstrip coupled lines and stronger coupling are achieved using this technique. A 20 dB initial coupler (over a fractional bandwidth of 35% with  $\pm 1$ dB ripple) is converted into 8 dB coupler with almost 3 times wider band by etching off a single unit cell of rectangular and meandered slot loop in the ground plane under the central part of the coupling region. Optimum DGS dimensions are related to coupler dimensions in easy to use design curves. An efficient technique for compensation of the significant unavoidable mismatch resulting from the presence of the DGS is applied and tested. Some coupler samples with different DGS are fabricated, measured, and compared with a conventional coupler counterpart to verify the simulation results and illustrate the improvements, very good agreements are observed.

**Index Terms**— Defected ground structures, directional coupler, microstrip, wideband.

## I. INTRODUCTION

Couplers are essential components for applications in virtually all RF and microwave transmission systems, such as power and VSWR measurements, signal sampling for monitoring or testing, equal or unequal power division, phase shifting (particularly  $90^\circ$  and  $180^\circ$ ), feed-forward

signal injection, isolation of signal sources. Other applications with the highest possible performance are particularly required in instrumentation, such as the new version of vector network analyzers require couplers with wide bandwidth, flat frequency response, and long-term stability [1].

In recent years, a growing research interest has been shown in applying various shapes of defected ground structures (DGS) to improve the performance of microwave circuits, such as microstrip filters and couplers. DGS are achieved by etching off a defected pattern from the ground plane of the microstrip line. Such structures disturb the current distribution in the ground plane and hence, introducing higher effective inductance and capacitance of the microstrip circuit, and reject certain frequency bands. A design of the lowpass filter using microstrip defected ground structure has been first proposed by Ahn et al. [2] in 2001. Numerous publications have applied the DGS in lowpass filter [2-6], and in directional coupler designs [7-10]. Hong et al. [11] proposed a general circuit model that represents varieties of DGS in either microstrip or coplanar waveguide (CPW).

It is commonly known that higher coupling in conventional microstrip couplers can be achieved by tightening the spacing between the coupled lines which is limited by fabrication tolerance. Sharma et al. [10] demonstrated an edge-coupled coupler with reasonable spacing between lines and improved coupling by introducing a rectangular slot in the ground plane under the coupler lines. Burokur et al. [7] realized a narrow band coupler by using the inverted slot split-ring resonators

(SSRR). Liu et al. [8] has proposed a microstrip coupler with complementary split-ring resonator (CSRR), to achieve a 3 dB coupling over a fractional bandwidth of only 38.1%. With utilizing the properties of electromagnetic bandgap structure (EBG), Wu et al. [9] improved the coupling of a microstrip coupler by using cascaded EBG and showed a broader coupling band.

Other works have used other methods rather than DGS such as inductor loading to enhance the directivity and the bandwidth as Seungku et al. [12] for a bandwidth of 16.3% at 2.4 GHz or using multi-section asymmetric directional coupler as Gruszczynski et al. [13] to achieve 4 GHz bandwidth at 3 GHz center frequency.

Dong et al. [14] has used a DGS technique on a CPW directional coupler design and achieved only 1 GHz bandwidth (50% fractional bandwidth at 2 GHz center frequency). Conventional edge-coupled microstrip coupler design, applying floating-plate overlay (not DGS), can be found in Kuo-Sheng et al. [15] for a one-section (one-stage) 3-dB and three-section (three-stages) 6 dB directional couplers over a bandwidth of 1 to 2 GHz (54% and 94% fractional bandwidth, respectively). Abbosh [16] demonstrated a 3 dB coupling coefficient over a wide bandwidth by converting an initial 7 dB conventional coupler, which implies a 4 dB coupling gain. This is achieved by applying a DGS of a floating potential plate in the ground plane. However, the coupled line spacing of only 0.13 mm still seems to be tight. The mismatch introduced by the DGS and restoring it to acceptable levels may also need to be addressed.

In this paper, a simplified approach, for systematic control of the coupler characteristics, is presented. This approach provides a much more relaxed line spacing and compensated mismatch caused by the presence of DGS. The DGS geometrical parameters are related to the geometry of any desired initial coupler through several extracted design curves which enables the designer to identify the trade-offs between geometry and performance parameters. The investigation includes DGS geometries from rectangular slot area to rectangular slot loop and meandered versions of slot loops. The mismatch caused by the DGS that deteriorates the reflection and isolation scattering parameters was compensated by inserting a narrow notch in the feed arms of the

initial coupler in addition to mitering the corners with the feed lines. Full-wave EM simulation tools [17-18] are used in the study. Samples of the proposed couplers are fabricated, measured, and compared and their results have very good agreements.

## II. DESIGN AND GEOMETRY

Before starting with the geometrical details of the coupler and related DGS design to be used in the simulations, it is useful to discuss some concepts of the DGS and its effects on the properties of the microstrip line.

### A. Design considerations

A DGS in the ground is a kind of slot, regardless of its shape: a line slot, rectangular slot area, slot loop, dumbbell etc., and single or periodic, all exhibit multi stop bands in frequencies [11].

It is known that the presence of the DGS modifies the properties of the microstrip line such as characteristic impedance and propagation constant. Thus, a disturbance of the already setup matching is expected. The simplest general equivalent circuit of a DGS can be presented in parallel *LC* circuit resonators, which can also be obtained from cutoff and attenuation frequencies obtained from the field analysis or the experimental measurement.

The coupled microstrip lines support two propagation modes denoted as even and odd modes. In the even mode, the electric field is symmetric, and the DGS may act as an open circuit, consequently slowing down the signal phase velocity, something like passing through a series stub. While in the odd mode, the electric field is asymmetric and the slot behaves something like a short circuit, where the signal can simply pass through without slowing down its phase velocity which is the same as if the DGS is absent. When the phase velocity decreases as is the case in the even mode, the effective dielectric constant increases. In this way, the microstrip properties are modified by the DGS, so the coupling coefficient may, also, be controlled by the shape and dimensions of the DGS. A simple equation illustrating such a control is given from the proportionality [19]

$$|S_{31}| \propto \Delta n_{eff} = \sqrt{\epsilon_{r_{effe}}} - \sqrt{\epsilon_{r_{effo}}}, \quad (1)$$

where  $|S_{31}|$  is the magnitude of the coupling coefficient, while the  $\epsilon_{r_{effe}}$  and  $\epsilon_{r_{effo}}$  are the effective dielectric constant for the even and odd modes, respectively.

### B. Design geometry

The initial microstrip coupler (without DGS) is designed using conventional synthesis technique [20-22]. The well known design steps are used assuming symmetrical two-line microstrip directional coupler. The coupler was designed on RT/Duroid 5880 ( $\epsilon_r = 2.2$ ,  $h = 1.5748$  mm) with -20 dB coupling coefficient at center frequency of 2 GHz.

The coupling level is deliberately chosen, so to obtain enough spacing and reasonable line width to ease the fabrication lithography process. The geometrical dimensions, Fig.1, are ( $W_C = 4.8$  mm), ( $S_C = 1.8$  mm), and ( $L_C = 36$  mm) which are the width of the lines in the coupled region, the separation between the coupled lines, and the coupling length of the coupler, respectively.

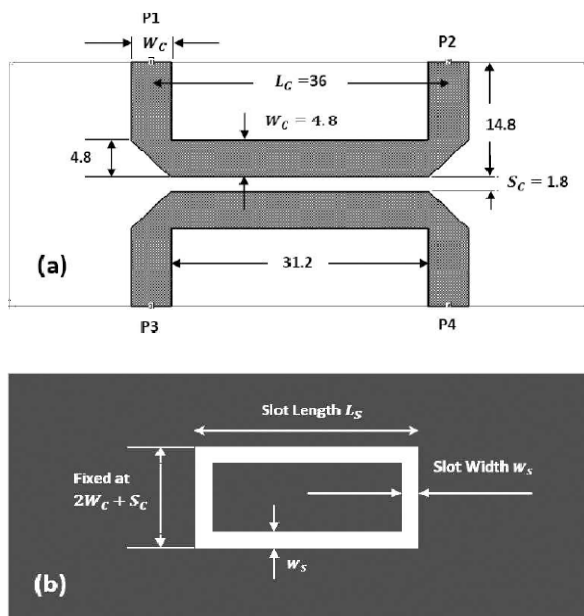


Fig. 1. Initial microstrip coupler with DGS. All dimensions are in mm. (a) Geometry of the -20 dB coupler. (b) DGS rectangular slot loop.

For preliminary investigation, the DGS structure, chosen to be applied with this initial coupler, is a rectangular slot loop shown in Fig. 1

(b). The parameters are denoted as: slot length ( $L_S$ ), slot width ( $W_S$ ), and the slot side ( $2W_C + S_C$ ) that is maintained fixed in all investigations. The other dimensions are made variables during the optimization process as will be shown in next sections.

### III. SIMULATION RESULTS

The simulated frequency response of the initial microstrip coupler without DGS, that has a finite ground plane, is shown in Fig. 2. It achieves -20 dB coupling around the operating frequency 2 GHz as specified with acceptable transmission, isolation, and reflection coefficients. The effect of varying the DGS slot loop length and width will be discussed next.

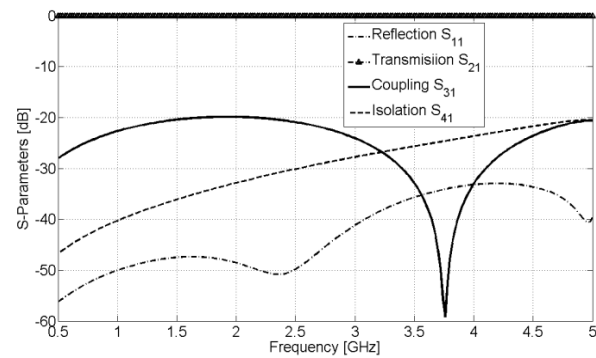


Fig. 2. Simulated S-Parameters of the -20 dB initial coupler without DGS, designed at 2 GHz.

#### A. Effect of the DGS slot loop dimensions

Preliminary investigations showed that a reasonable slot loop width of ( $W_S = 1.2$  mm) can be used as a starting parameter. The slot loop length ( $L_S$ ) is then altered from zero up to nearly the coupling length ( $L_C$ ). Note that when ( $L_S = 0$ ), the DGS vanishes and the coupler is returned back to its original initial microstrip structure.

The DGS geometrical parameters are illustrated in Fig. 3, where two investigations will be conducted to gain insight in designing the DGS and to achieve the optimal design in terms of all scattering parameters. In Fig. 3 (a), the slot loop width ( $W_S$ ) is fixed at 1.2 mm, while in Fig. 3 (b), the slot length ( $L_S$ ) is fixed at 24 mm.

For convenience of extracted data, normalized values are used such as normalized slot length to coupling length ( $L_S / L_C$ ) and normalized slot width to coupled line width ( $W_S / W_C$ ). This is

essential to relate the DGS dimensions with the initial coupler dimensions. Figure 4 illustrates the simulated S-parameters against the normalized slot length to coupling length ( $L_S / L_C$ ) at fixed ratio of slot width to coupling width ( $W_S / W_C = 0.25$ ). Figure 5 illustrates the simulated S-parameters against the normalized slot width to coupling width ( $W_S / W_C$ ) at fixed ratio of slot length to coupling length ( $L_S / L_C = 1$ ).

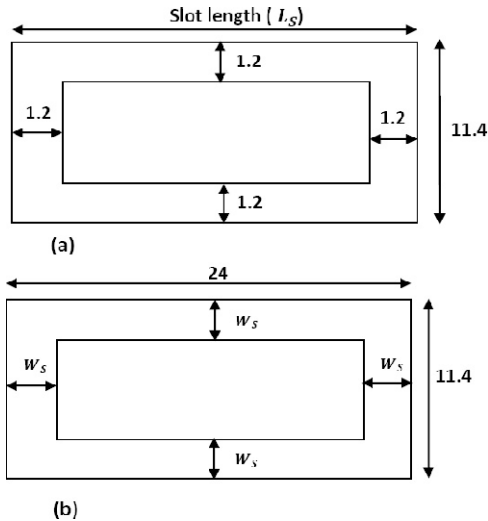


Fig. 3. DGS geometry. (a) Variation of ( $L_S$ ) at fixed ( $W_S$ ). (b) Variation of ( $W_S$ ) at fixed ( $L_S$ ).

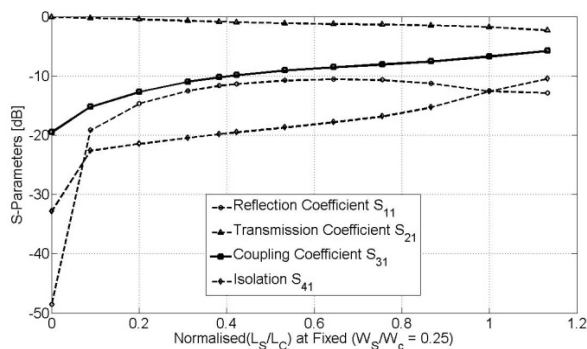


Fig. 4. The S-parameters against normalized ( $L_S / L_C$ ) at fixed ratio ( $W_S / W_C = 1/4$ ).

From these plots (Fig. 4 and Fig. 5), although an immediate increase in the coupling from -20 dB to around -7 dB is observed, it can be clearly seen that this increase in coupling is associated with a significant deterioration of reflection and isolation coefficients  $S_{11}$  and  $S_{41}$ . Such deterioration would

make the coupler useless. This is due to a significant mismatch caused by applying the DGS beneath the coupler which confirms the concepts mentioned in the design considerations in Section II. A. However, it can also be seen that the effect of slot length variations is stronger than the effect of the slot width. This may be due to the fact that increasing the slot length, actually increases the metallic conductor area beneath the coupler lines and affects the electric field distribution of the structure; hence, the odd mode capacitance of the structure will increase. Increasing the slot width, on the hand, reduces the conductor area beneath the coupler lines. As a result, an opposite effect occurs on both even and odd modes capacitances (see also the discussions in Section II).

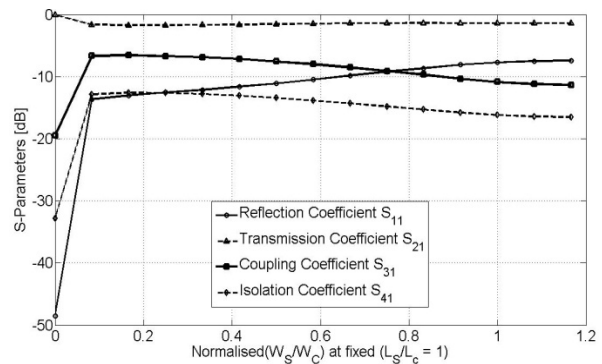


Fig. 5. The S-parameters against ( $W_S / W_C$ ) at fixed ratio of ( $L_S / L_C = 1$ ).

To complete this preliminary study, the effect of slot length and width variations on the coupler fractional bandwidth (B%) are shown in Fig. 6. In fact, the very large fractional bandwidth of the coupling above 90% is associated with the worst  $S_{11}$  and  $S_{41}$ , as expected. Also, the slot length effect on the bandwidth is much stronger than the slot width effect.

It should be noted that the variations of S-parameters due to slot dimensions are larger in the higher frequency region than in the lower frequency region. This may be due to the difference in phase velocities of the odd and even modes of the coupler.

To acquire better insight on the extent of the resulting mismatch in the reflection coefficient  $S_{11}$  (even with the improvement of the coupling coefficient  $S_{31}$  over a wide frequency band),

several simulations for  $S_{11}$  and  $S_{31}$  responses, are plotted in Fig. 7 to illustrate these effects.

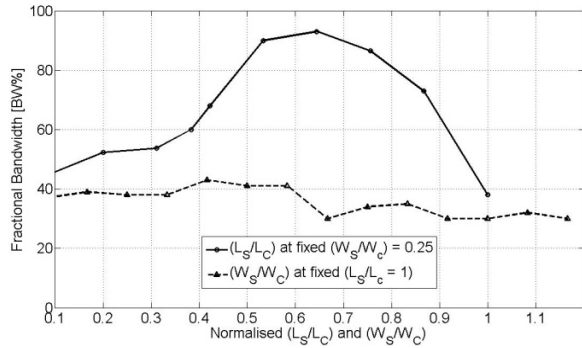


Fig. 6. Fractional bandwidth (B%) against  $(L_S / L_C)$  and  $(W_S / W_C)$  at fixed ratios of  $(W_S / W_C = 1/4)$  and  $(L_S / L_C = 1)$  respectively.

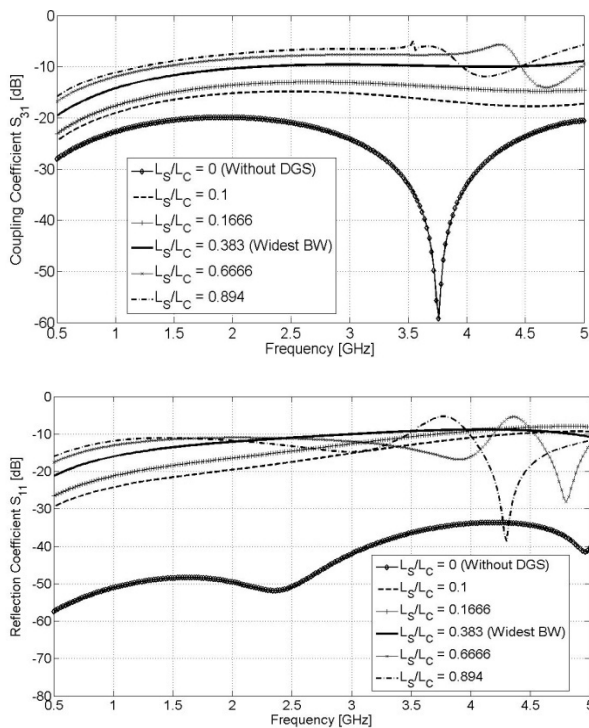


Fig. 7. The coupling and reflection coefficients against frequency at different values  $(L_S / L_C)$  at fixed ratio of  $(W_S / W_C = 1/4)$ .

**B. Mismatch compensation of the DGS coupler**

The presence of the DGS modifies some properties of the microstrip line including the coupling coefficient, but at the same time deteriorates both the reflection coefficient  $S_{11}$  and

isolation coefficient  $S_{41}$ . Thus, the already matched initial coupler is expected to deteriorate its reflection  $S_{11}$  and isolation coefficient  $S_{41}$ , although the coupling bandwidth has improved. To restore the  $S_{11}$  and  $S_{41}$  Performance, while maintaining a wide bandwidth and relatively flat coupling response, mismatch compensation should be achieved. Thus, the coupler feed arms are modified with a narrow notch and increased depth of the corner mitering as shown in Fig. 8 (a). Figure 8 (b) shows the DGS geometrical parameters used in the subsequent simulations. Therefore, it is important to investigate the impact of this mismatch compensation method on the other scattering parameters of the coupler.

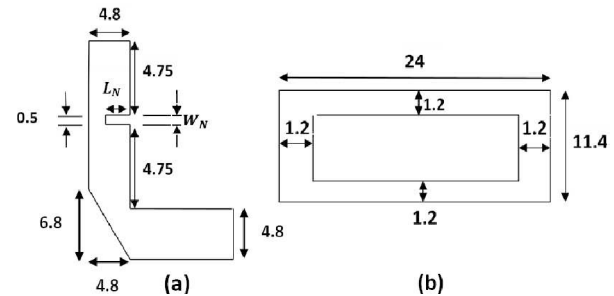


Fig. 8. Geometry of the notch length  $(L_N)$  and associated DGS of the coupler.

The effect of the notch feed lines and mitered corners, on S-parameters of the modified coupler, is shown in Fig. 9. The normalized notch length to coupler width  $(L_S / W_C)$  is varied at fixed notch width  $(W_N / W_C \approx 1)$ .

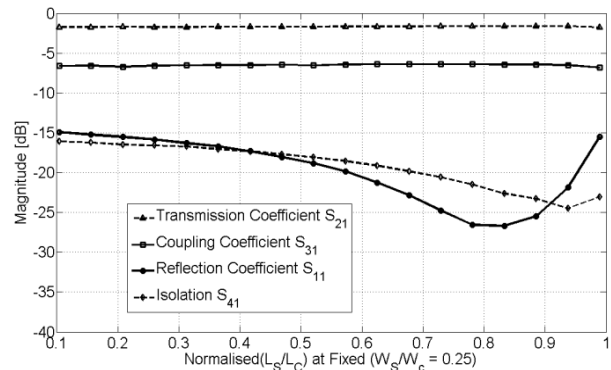


Fig. 9. Effect of the notch and mitering on the scattering parameters of the modified coupler, against  $(L_S / W_C)$  at fixed ratio of  $(W_N / W_C \approx 1)$ .

The improvement on  $S_{11}$  and  $S_{41}$  is evident in the limits ( $0.65 \leq L_N / W_C \leq 0.85$ ), while the other parameters remain almost unchanged. The optimum notch length is chosen to be 4 mm, i.e. ( $L_N / W_C = 0.833$ ). That gives a broader coupling coefficient.

The modified coupler is shown in Fig. 10, while the S-parameters with respect to ( $L_S / L_C$ ) at ( $W_S / W_C = 1/4$ ) are shown in Fig. 11, where the notch is fixed at length of 4 mm and width of 0.5 mm. From Fig. 11, it can be seen that when the ratio of ( $L_S / L_C = 2/3$ ), a better performance of  $S_{11}$  and  $S_{41}$  has been occurred, so the slot length ( $L_S$ ) will be equal to 24 mm. This value is adopted as optimum for the investigations.

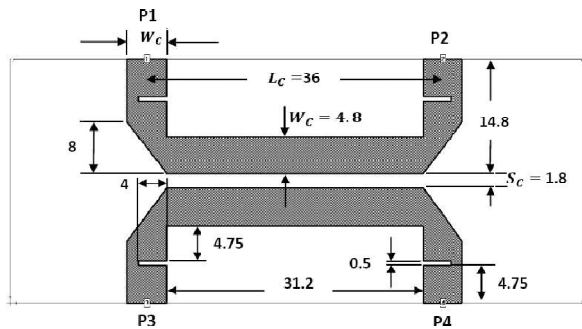


Fig. 10. Geometry of the modified initial coupler with a notch in feed arms. All dimensions are in mm.

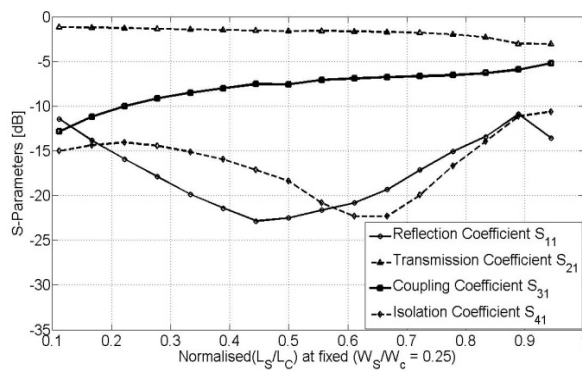


Fig. 11. Variation of S-parameters of the modified coupler against ( $L_S / L_C$ ) at fixed ( $W_S / W_C = 1/4$ ). The notch dimensions are 4 mm x 0.5 mm.

Now, it is worth monitoring the variations of fractional bandwidth (B%) for the coupler (Fig. 10) against the ratios ( $L_S / L_C$ ), and ( $W_S / W_C$ ) at fixed ratios ( $W_S / W_C = 1/4$ ), and ( $L_S / L_C = 2/3$ )

respectively. These relationships are illustrated in Fig. 12 where the effect on (B%) by varying the slot width is much smaller than the effect of varying the slot length. The best (B%) is somewhere about a value of ( $L_S / L_C = 2/3$ ) at fixed value of ( $W_S / W_C = 1/4$ ), i.e. a slot length of  $L_S = 24$  mm and slot width of  $W_S = 1.2$  mm. These values are adopted for the coupler to be fabricated and measured.

The variation of S-parameters of the coupler (Fig. 10) against normalized slot width ( $W_S / W_C$ ) at fixed ratio of slot length ( $L_S / L_C = 2/3$ ), is shown in Fig. 13. The variations are relatively slight in comparison to those due to slot length variation.

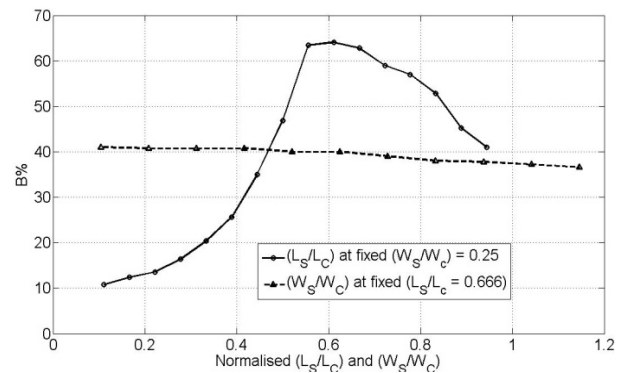


Fig. 12. Variation of (B%) of the coupler (Fig. 10), against ( $L_S / L_C$ ), and ( $W_S / W_C$ ) at fixed ratios of ( $W_S / W_C = 1/4$ ), and ( $L_S / L_C = 2/3$ ), respectively.

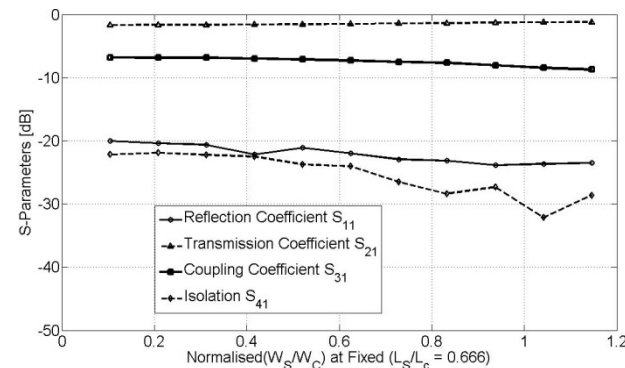


Fig. 13. The S-parameters of the coupler (Fig. 10), against normalized slot width ( $W_S / W_C$ ) at fixed ratio of slot length ( $L_S / L_C = 2/3$ ).

## IV. FABRICATIONS AND MEASUREMENTS

### A. Rectangular slot loop example

Following the design considerations in Section II and simulation results, summarized in several useful design curves, the microstrip coupler shown in Fig. 10 was fabricated, using thin film technology and photolithographic techniques. The substrate used is Rogers RT/Duroid 5880 ( $\epsilon_r = 2.2$ ,  $h = 1.5748$  mm). The photo of the realized coupler (coupler-1) with DGS is shown in Fig. 14. The simulated and measured S-parameters of this coupler are presented in Fig. 15.

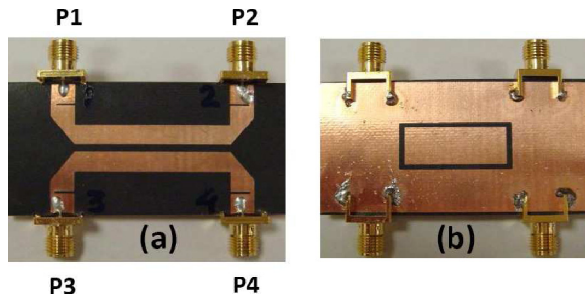


Fig. 14. Photo of the measured example coupler-1. (a) The top layer. (b) The bottom DGS layer.

The simulated and measured S-parameters are in a good agreement. The measured  $S_{31}$  is smoother than the simulated response above 3 GHz, which may be due to parasitic radiation effects from the DGS, not taken into account by the simulation tools for the surroundings of the coupler. In addition, there are tolerances between the box shield used in the simulation tools and the microstrip test fixture used in measurements.

The measured  $S_{11}$  and  $S_{41}$  are all below 20 dB in the coupling bandwidth, and better than the simulated counterparts at certain frequencies. However, the ripple of  $S_{11}$  seems stronger than the simulated response.

### B. Meandered slot loop example

Meandering the DGS slot loop actually adds more bends in the structure and hence its size can be reduced while maintaining the same total length and area.

More bends, on the other hand, are expected to increase the parasitic capacitances. Reducing the DGS size would allow applying more DGS cells in the available ground area.

Several publications [7, 9, 11] have shown that multiple cells (or periodic DGS structure) are another way to improve the coupling performance. Thus, testing a single cell of such a meandered slot loop is useful to explore such effects on the coupling coefficient  $S_{31}$  and its fractional bandwidth (B%), while maintaining acceptable levels of  $S_{11}$  and  $S_{41}$ . Meandering can, also, be made multiple on all sides of the slot structure if needed.

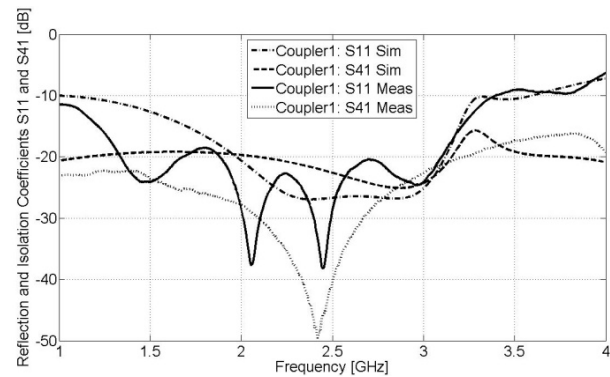
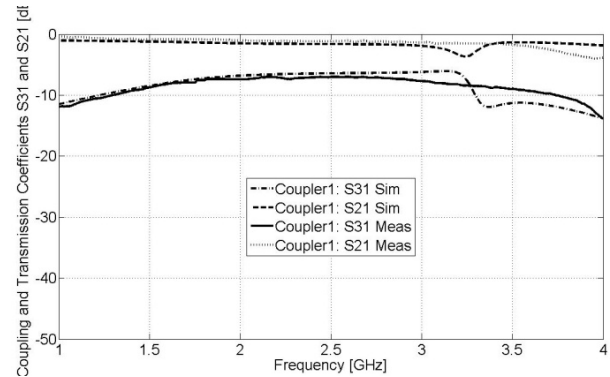


Fig. 15. Simulated and measured S-parameters of DGS coupler (coupler-1).

Two microstrip directional couplers with different meandered slot dimensions were fabricated according to the geometries shown in Fig. 16. The top layer of the initial coupler geometry (Fig. 16 (a)) is used for the two different DGS structures (Fig. 16 (b) and (c)).

Photos of the two fabricated couplers are shown in Fig. 17. For convenience, the top and bottom layers of Fig. 16 (a) and (b) are assigned as coupler-2, while Fig. 16 (a) and (c) as coupler-3. For coupler-2, the simulated and measured frequency responses of S-parameters are compared in Fig. 18, where a good agreement was observed.

The coupler achieves 2.5 GHz bandwidth with a coupling coefficient ( $S_{31} = -7 \pm 1$ dB). This would correspond to a fractional bandwidth of 125% at a center frequency of 2 GHz. However, if we consider the associated reflection and isolation coefficients  $S_{11}$  and  $S_{41}$  with acceptable values below -15 dB and -20 dB, respectively, the useful bandwidth would be reduced to around 95%.

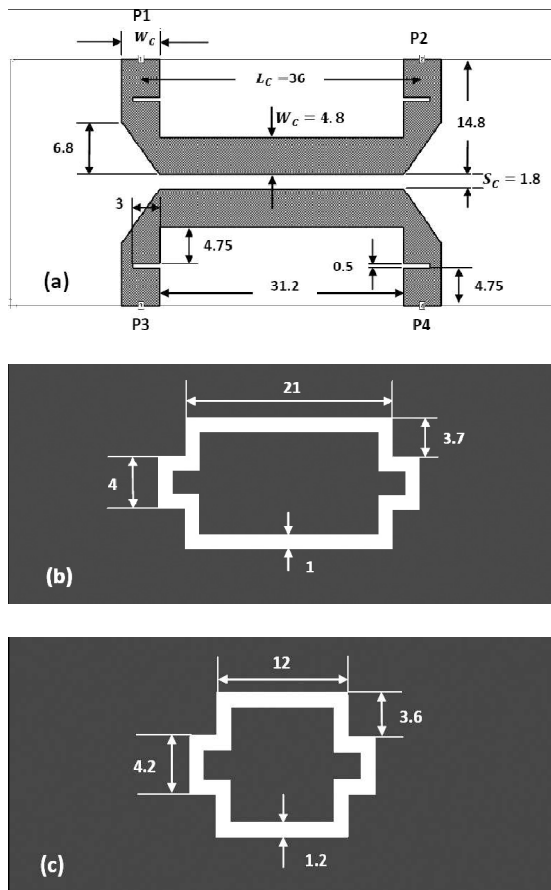


Fig. 16. Geometric dimension of the fabricated meandered DGS couplers 2 and 3. (a) The top layer geometry used for both couplers. (b) DGS geometry of coupler 2. (c) DGS geometry of coupler 3. All dimensions are in mm.

For coupler-3 with smaller DGS meandered slot dimensions, the simulated and measured S-parameters are compared in Fig. 19. Good agreement was observed, but the coupling coefficient for this coupler is slightly weaker ( $S_{31} = -10 \pm 1$ dB) than in coupler-2. The sharp drop (observed in coupler-2) in the coupling level beyond 4 GHz is not observed for coupler-3.

The measured  $S_{11}$  is still below -15 dB in the entire lower frequency region up to 3 GHz, beyond which, a sharp rise is seen. On the other hand, the measured  $S_{41}$  is below 25 dB in most of the frequency region, which is better than  $S_{41}$  in coupler-2.

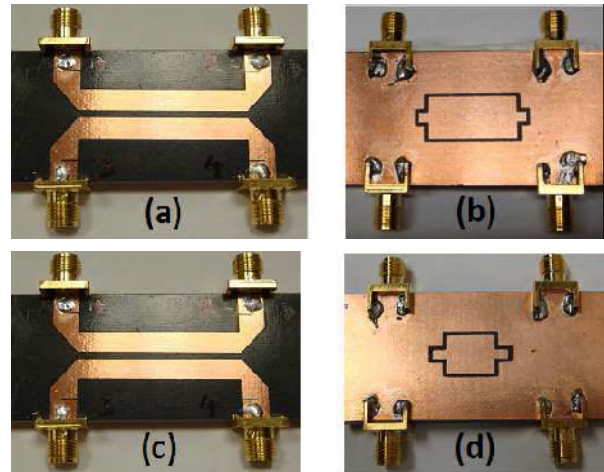


Fig. 17. Photos of the realized and measured couplers, (a) & (b) for coupler-2 while (c) & (d) for coupler-3.

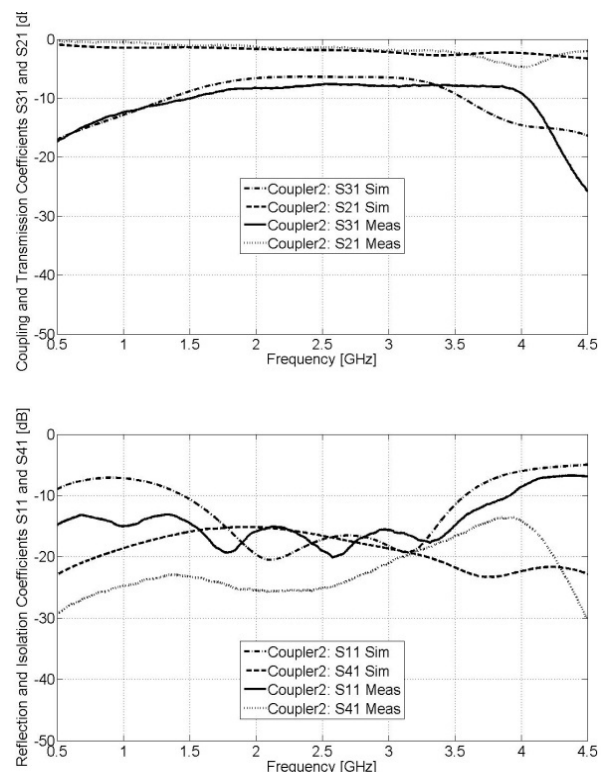


Fig. 18. Measured and simulated S-parameters of the DGS coupler-2.

It can be seen that meandering the DGS slot loop does not show significant effect on the overall performance of the desired parameters, although it affects the reflection and isolation positively and slightly decreases the coupling level.

In general, the measurements confirm the approach undertaken to identify trade-offs in selecting the design geometry, so to achieve the desired coupler response, in terms of the coupling bandwidth, flatness and reasonable levels of reflection and isolation coefficients.

The achieved results for the investigated structures and design curves can be applied to other frequencies of interest, if scaling theory is properly applied to all geometrical and substrate parameters.

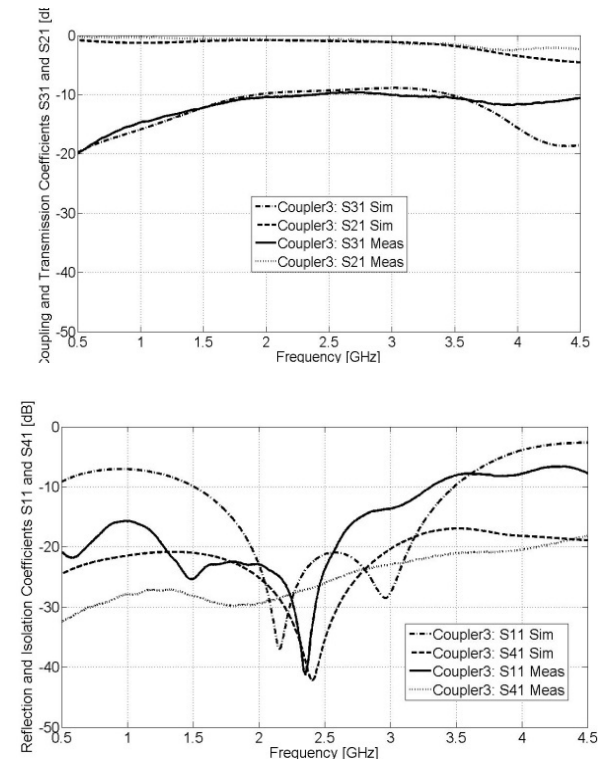


Fig. 19. Simulated and measured S-parameters of the DGS coupler-3.

## V. CONCLUSION

Various microstrip directional couplers, composed of DGS shapes, ranging from slot area to slot loop, were studied. Three different samples of DGS couplers were fabricated and measured. The measured responses were in good agreement

with the specified parameters and the full-wave simulations. The results showed that the coupling level can be raised from -20 dB to around -8 dB over a relatively wide bandwidth of 3 GHz, which corresponds to more than 95% fractional bandwidth ( $\pm 1$  dB ripple) and acceptable levels of reflection and isolation below -15 dB and -20 dB, respectively).

Such results are not achievable with a conventional microstrip directional coupler, having a reasonable spacing between the coupled lines, crucial for fabrication lithography techniques. Various effects of the DGS on the coupler performance were investigated and many useful design curves were extracted. The study showed that the coupling bandwidth can be increased significantly, but this is limited by a deterioration of the reflection and isolation coefficients. A well-matched microstrip coupler exhibited a large mismatch when the DGS is present. A method is applied to restore the matching to acceptable levels, but with some reduction in the bandwidth. The unit cell DGS structure may be applied in other shapes or multiples of such a cell for further improvement of the coupling. If the initial coupler is designed with -15 or -10 dB coupling, the described DGS is expected to raise the coupling to much tighter levels.

## ACKNOWLEDGMENT

The authors would like to acknowledge the assistance in fabrication and measurement provided by PSATRI (Prince Sultan for Advanced Technology Research Institute), King Saud University, Saudi Arabia.

## REFERENCES

- [1] Technology report, "Couplers remain important products, using new manufacturing techniques," High Frequency Electronics, Summit Technical Media, LLC, pp. 42–44, January, 2003.
- [2] D. Ahn, J. S. Park, C. S. Kim, J. Kim, Y. Qian, and T. Itoh, "A design of the lowpass filter using the novel microstrip defected ground structure," *IEEE Trans. on Microwave Theory and Techniques*, vol. 49, no. 1, pp. 86–93, 2001.
- [3] A. B. A. Rahman, A. K. Verma, A. Boutejdar, and A. S. Omar, "Control of bandstop

- response of Hi-Lo microstrip low-pass filter using slot in ground plane,” *IEEE Trans. on Microwave Theory Tech.*, vol. 52, no. 3, pp. 1008–1013, 2004.
- [4] J. -X. Chen, J. -L. Li, K. -C. Wan, and Q. Xue, “Compact quasi-elliptic function filter based on defected ground structure,” *IEE Proc.-Microwave Antennas propagation*, vol. 153, no. 4, pp. 320–324, 2006.
- [5] P. Vagner and M. Kasal, “Design of novel microstrip low-pass filter using defected ground structures,” *Microwave and Optical Technology Letters*, vol. 50, no. 1, pp. 10–13, 2007.
- [6] A. S. Mohra, “Compact lowpass filter with sharp transition band based on defected ground structures,” *Progress In Electromagnetics Research Letters*, vol. 8, pp. 83–92, 2009.
- [7] S. N. Burokur and M. Latrach, “A novel type of microstrip coupler utilizing a slot split-ring resonators defected ground plane,” *Microwave Opt. Technol. Lett.*, vol. 48, no. 1, pp. 138–141, 2006.
- [8] K. Y. Liu, C. Li, and F. Li, “A new type of microstrip coupler with complementary splitting resonator (CSRR),” *PIERS Online*, vol. 3, no. 5, pp. 603–606, 2007.
- [9] R.-X. Wu, X.-Y. Ji, R.-F. Chen, and Y. Poo, “A Novel microstrip coupler with EBG structures,” *Asia-Pacific Microwave Conference, APMC08*, Macau, pp. 1–4, 2008.
- [10] R. Sharma, T. Chakravarty, and S. Bhooshan, “Design of a novel 3db microstrip backward wave coupler using defected ground structure,” *Progress In Electromagnetics Research*, vol. 65, pp. 261–273, 2006.
- [11] J.-S. Hong and B. M. Karyapudi, “A General circuit model for defected ground structures in planar transmission lines,” *IEEE microwave and wireless components letters*, vol. 15, no. 10, pp. 706–708, 2005.
- [12] S. Lee and Y. Lee, “A design method for microstrip directional couplers loaded with shunt inductors for directivity enhancement,” *IEEE Trans. Microw. Theory Tech.*, vol. 58, no. 4, pp. 994–1002, 2010.
- [13] S. Gruszczynski and K. Wincza, “Broadband multisection asymmetric 8.34-dB directional coupler with improved directivity,” *Proceedings of Asia-Pacific Microwave Conference*, 2007.
- [14] K. Dong-Joo, J. Yongwoo, K. Jung-Hoon, K. Jong-Hwa, K. Chul-Soo, L. Jong-Sik, and A. Dal, “A novel design of high directivity CPW directional coupler design by using DGS,” *IEEE, MTT-S Int. Microw. Symp. Dig.*, pp. 1239–1243, Long Beach, Ca, USA, 1995.
- [15] C. Kuo-Sheng, M. Ming-Chuan, C. Yi-Ping, and C. Yi-Chyun, “Closed-form equations of conventional microstrip couplers applied to design couplers and filters constructed with floating-plate overlay,” *IEEE Trans. Microw. Theory Tech.*, vol. 56, no. 5, pp. 1172–1179, 2008.
- [16] A. M. Abbosh, “Broadband parallel-coupled quadrature coupler with floating-potential ground plane conductor,” *Microwave and Optical Technology Letters*, vol. 50, no. 9, pp. 2304–2307, 2008.
- [17] Sonnet suit EM field solver software, Version: 12.56, North Syracuse, NY, www.sonnetsoftware.com.
- [18] IE3D EM Simulation and Optimization Package, Version 11.5, CA 94538, U.S.A, www.zeland.com.
- [19] UCLA research program in electrical engineering, “Application of defected ground structure in Microstrip line forward coupler,” <http://www.mwlab.ee.ucla.edu/>, 2003.
- [20] D. M. Pozar, *Microwave Engineering*, 3rd Ed., Wiley-Interscience, New York, 2005.
- [21] T. C. Edwards, *Foundations for Microstrip Circuit Design*, Wiley-Interscience, Chichester, 1981.
- [22] A. Eroglu and J. Kyoon Lee, “The complete design of microstrip directional couplers using the synthesis technique,” *IEEE Transactions on Instrumentation and Measurement*, vol. 57, no. 12, pp. 2756–2761, 2008.



**Ayman S. Al-Zayed** Received the B.Eng. (Honours) degree in Communication and Electronic Engineering from the University of Northumbria at Newcastle in 1995. In 2000, he obtained the M.S. degree in Electrical Engineering from the University of Hawaii at Manoa. In 2004, he earned the Ph.D.

degree in Electrical Engineering from North Carolina State University. In February, 2004, he joined the Department of Electrical Engineering at Kuwait University where he is currently an Assistant Professor. His research interests include microwave and millimeter-wave active and passive devices, power combining, quasi-optical devices, antennas, phased arrays and radars.



**Zuhair M. Hejazi** He is an Associate Professor of Telecommunication Engineering. He received the Diploma Degree in Radio Engineering- Radar & Radio Navigation from the Technical University of Sofia in 1981. The M.Phil. and Ph.D. degrees, from Bradford University- UK, in 1995 and 1998, respectively. From 1985 to 1988, he was working in the Quality Control of Digital Radio Link Systems and CAD of Microwave Components for Siemens and two other Companies in München, Germany. From 1990 to 1993, he was working as a Research and Teaching Assistant in the Hijawi Faculty for Engineering Technology, Yarmouk University, Jordan, where he served later as a Faculty Member, Assistant Dean and Chair of the Telecommunications Engineering Department. Recently, he served in Middle East College of Information Technology (MECIT), Muscat-Oman for two years as a faculty and HoD of the Electronics and Telecommunication Department. Currently, he is a faculty with the EE Department, College of Engineering, King Saud University, Riyadh, KSA. His research interests are mainly in microwave devices, planar filters, couplers, and antennas.



**Ashraf Shouki Mohra** Was born in Cairo, Egypt. Each of M.S. and Ph.D. degree were received in Electronics and Communications from Ain Shams University in 1994 and 2000, respectively. He worked in the Electronics Research Institute, Ministry of scientific research and technology, Cairo, Egypt. He has worked on the analysis and design of microstrip circuits, such as couplers, filters, six-port reflectometers, defected ground structures, metamaterials, etc. He was promoted to associate professor at Electronics Research Institute on March 2006. Now, he is with EE Dept, College of Engineering, King Saud University. His current fields of interests are concerned with the computer aided design of microwave and millimeter-wave wide-band planar circuits and microstrip antennas using photolithographic technique and thin film technology.